Earth, Planets and Space

FULL PAPER

Open Access

Double seismic zone and seismicity in the mantle wedge beneath the Ogasawara Islands identified by an ocean bottom seismometer observation

Kenji Nakata[1*], Akio Kobayashi[1], Akio Katsumata[1], Fuyuki Hirose[1], Takahito Nishimiya[1], Kazuhiro Kimura[2], Hiroaki Tsushima[2], Kenji Maeda[2], Hisatoshi Baba[3], Noritaka Hanamura[4], Chisato Yamada[5] and Masashi Kanezashi[6]

Abstract
Around the Ogasawara Islands, only a few seismic stations in the area can be used to determine the hypocenters of regional earthquakes; thus, hypocenter location precision tends to be low. To more precisely determine hypocenter locations, we deployed a temporary seismic observation network of pop-up ocean bottom seismometers around the Ogasawara Islands from July to October 2015. We identified a double seismic zone in the 70–200 km depth range associated with the subducting Pacific slab. The slab-normal distance between the two planes of the double seismic zone is about 30–35 km, similar to such distances observed along the Japan and Mariana trenches. Furthermore, we found unusual seismicity in the mantle wedge at 20–50 km depth beneath the Ogasawara trough that might be related to structure formed at the onset of the oceanic slab subduction. The hypocenters determined from the ocean bottom seismometer observation were horizontally separated by a few tens of kilometers from hypocenters published by the *Seismological Bulletin of Japan*. USGS locations (Preliminary Determination of Epicenters) seem to be offset westward about 30 km compared with the locations determined in this study.

Keywords: Ocean bottom seismometer, Izu-Ogasawara, Double seismic zone, Mantle wedge, Precision of hypocenter

Introduction

The Japan Meteorological Agency (JMA) compiles seismic data from many sources and publishes hypocenter data in the *Seismological Bulletin of Japan* (SBJ) with the help of the Ministry of Education, Culture, Sports, Science and Technology of Japan. Although inland areas of Japan are covered by a dense seismic network, the number of seismic stations is limited in small island regions far from the main islands of Japan. In the Ogasawara Islands, in particular, there are only three seismic stations, located almost in a line on Chichijima, Hahajima, and Iwoto islands; the next closest station is on Aogashima, an island 600 km north of Chichijima. Hypocenters in the Ogasawara region are determined by using data from this sparse local network together with data from some stations on Honshu and other Japanese islands. Epicenters in the Ogasawara region published by SBJ are often located several tens of kilometers east of corresponding epicenters in the Preliminary Determination of Epicenters bulletin (PDE), published by the US Geological Survey (USGS) (Fig. 1).

In the Ogasawara region, a number of reflection and refraction seismic surveys have been conducted with ocean bottom seismometers (OBSs) (e.g., Takahashi et al. 2009). One survey, for example, deployed OBSs along a 580-km-long baseline and estimated the

*Correspondence: knakata@mri-jma.go.jp
[1] Meteorological Research Institute, Japan Meteorological Agency, 1-1 Nagamine, Tsukuba, Ibaraki 305-0052, Japan
Full list of author information is available at the end of the article

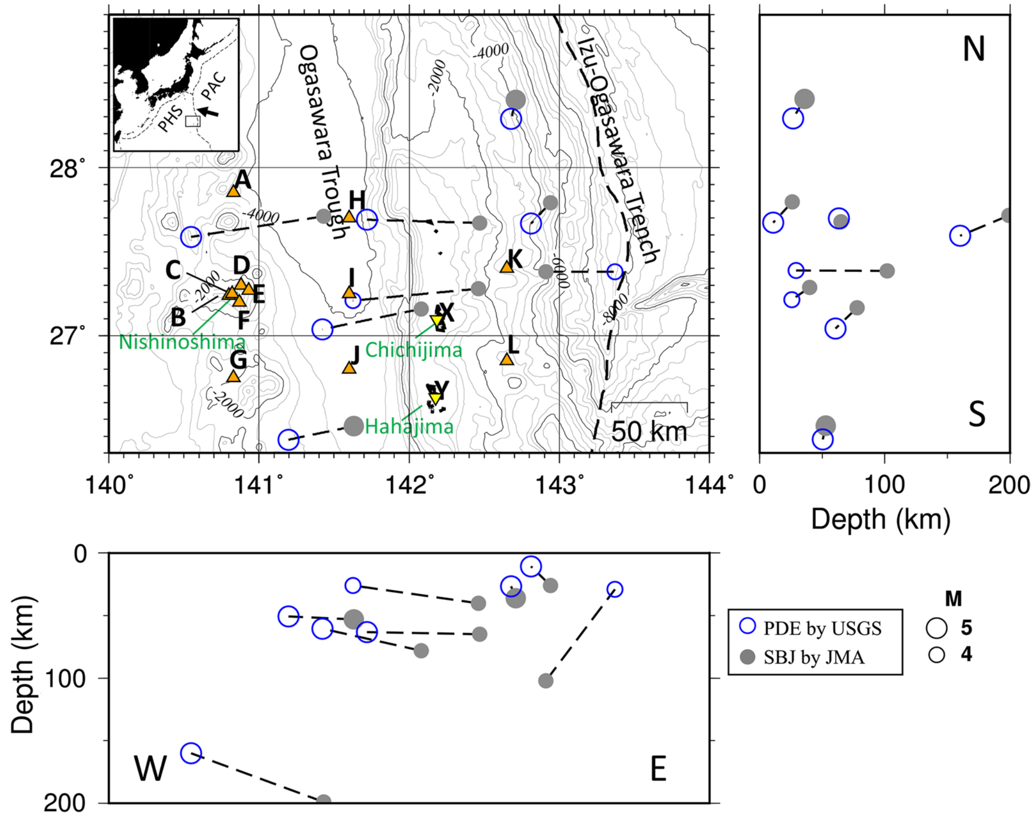

Fig. 1 Comparison of hypocenter locations observed in 2013: gray circles, SBJ; blue circles, PDE. The locations of OBSs (orange triangles) and the land stations on Chichijima and Hahajima (inverted yellow triangles) used in this study are also shown. The bathymetry (gray lines) is shown with a contour interval of 500 m. The inset map shows the area of this study and the direction of movement (arrow) of the Pacific plate (PAC) relative to the Philippine Sea plate (PHS)

velocity structure down to 30 km below the seafloor (Kodaira et al. 2010). However, no OBS observations targeting natural earthquakes are conducted in this area.

The subduction of the Pacific plate (PAC) beneath the Philippine Sea plate along the Izu-Ogasawara trench has recently led to notable seismic activity, including a normal-fault earthquake (M_w 7.3) on 22 December 2010 (JMA 2010) and a deep-focus earthquake (M_w 7.9) on 30 May 2015 (JMA 2015). Along the Izu-Ogasawara trench, the occurrence of shallow earthquake greater than M 8 has not been known. Scholz and Small (1997) suggested that great earthquakes might occur where the Ogasawara Plateau is subducting beneath the Hahajima island group because of increase in interplate seismic coupling caused by seamount subduction. Ishibashi and Harada (2013) suggested a possibility that the source area of the 1605 Keicho earthquake may have been along the Izu-Ogasawara trench. Knowledge of the precise locations of seismic activity in this area could thus provide important information about future great earthquakes.

In this study, we determined the precise distribution of earthquake hypocenters with a pop-up OBS network that was deployed around the Ogasawara Islands for about three months in 2015. We aimed to grasp a wide range of seismic activity in the Ogasawara region with a horizontal distance of about 150 km and a depth down to about 200 km by using an observation network with the observation station intervals of 50 to 100 km.

Observation with pop-up OBSs

The OBS seismic network was deployed from 15 July to 10 October 2015 by R/V *Keifu-Maru*, a JMA research vessel. Twelve OBSs (stations A–L) were deployed in a 200 km × 100 km area, with five of them (stations B–F) deployed in the vicinity of Nishinoshima volcano (Table 1, Fig. 1). Data from OBSs, along with data recorded by the permanent land stations on Chichijima (station X) and Hahajima (station Y), were used for hypocenter determination. The horizontal coordinates of the OBSs were estimated by acoustic ranging, which usually has a location error of 20–30 m (Yamazaki 2011). Each

Table 1 Parameters of OBS stations used in this study

Station	Latitude (N)		Longitude (E)		Depth (m)	Observation period	ΔTps-p (s)	Pcor (s)	Scor (s)	σ_p (s)	σ_s (s)
	(°)	(min)	(°)	(min)							
A	27	51.0	140	49.7	3270	15 Jul. to 3 Oct. 2015	0.99	0.070	− 0.319	0.281	0.462
B	27	14.3	140	48.0	1219	21 Jun. to 28 Sep. 2015	0.95	1.274	0.296	0.092	0.000
C	27	15.1	140	49.4	944	21 Jun. to 2 Oct. 2015	0.86	1.493	2.594	0.141	0.246
D	27	17.8	140	52.6	1139	21 Jun. to 13 Sep. 2015	0.84	1.387	2.167	0.078	0.301
E	27	16.0	140	55.9	1206	21 Jun. to 28 Sep. 2015	1.04	1.248	1.802	0.188	0.532
F	27	12.2	140	52.2	922	21 Jun. to 18 Sep. 2015	1.11	1.517	1.192	0.288	1.527
G	26	45.0	140	49.8	2127	15 Jul. to 9 Oct. 2015	0.93	0.448	0.233	0.209	0.462
H	27	42.1	141	36.0	4144	15 Jul. to 23 Sep. 2015	1.28	− 0.473	− 1.900	0209	0.430
I	27	15.1	141	36.1	4043	15 Jul. to 5 Oct. 2015	0.60	− 0.451	− 1.650	0.209	0.534
J	26	48.1	141	36.0	3751	15 Jul. to 10 Oct. 2015	1.13	− 0.890	− 2.064	0.204	0.391
K	27	24.0	142	39.0	2783	15 Jul. to 4 Oct. 2015	0.72	0.160	0.418	0.228	0.589
L	26	51.0	142	38.9	2756	15 Jul. to 9 Oct. 2015	0.85	− 0.165	− 0.703	0.352	0.737
X (Chichijima)	27	5.7	142	11.1	− 145	–	–	1.574	3.397	0.349	0.690
Y (Hahajima)	26	38.0	142	10.5	− 108	–	–	1.194	2.521	0.515	0.631

ΔTps-p, arrival-time difference between the PS and P phases; Pcor, final station correction for the P phase; Scor, final station correction for the S phase; σ_p, standard deviation of the P-phase arrival time; σ_s, standard deviation of the S-phase arrival time

OBS consisted of a three-component seismometer with a natural period of 4.5 Hz (installed on a gimbal with oil-damping) and a hydrophone. Data at 16-bit resolution were continuously recorded at a sampling rate of 100 Hz. The difference between the clock time of each OBS and the Global Positioning System timing signal was measured before installation and after recovery of each OBS; then the OBS clock times were corrected by assuming that the time-shift rate was constant.

Hypocenter determination

Events were detected by applying the short-term-average/long-term-average (STA/LTA) method (Urabe and Hirata 1984) to the continuous record of seismic data from nine seismic stations (A, G–L, X, and Y; Fig. 1). Data recorded at stations B–F, close to Nishinoshima volcano, were excluded from the STA/LTA analysis because of the high level of volcanic activity during the OBS deployment period, but they were used to hypocenter determination. We set the decay constants for STA and LTA calculation at 2 and 60 s, respectively. When the STA/LTA exceeded a value of 3.0, detection status was turned on. When STA/LTA fell below 2.0, the status was turned off. A continuous ON status for more than 5 s was judged as a triggered event. These processes were performed at each observation station. The triggered event at only one station may be a noise or a small earthquake for which the hypocenter cannot be determined. Therefore, we selected the triggered events which got on at two or more stations simultaneously within 20 s and detected 1601 events as candidates for earthquake events. The WIN system was used to pick seismic wave onset times and maximum amplitudes (Urabe and Tsukada 1992). Examples of seismic records are shown in Fig. 2. Hypocenters of earthquakes for which one or more P-wave arrivals and five or more total P- and S-wave arrivals were detected were estimated with the HYPOMH program (Hirata and Matsu'ura 1987). We assumed a one-dimensional P-wave velocity structure based on the results of a seismic survey by Takahashi et al. (2009) (Fig. 3). The S-wave velocity was assumed to be 1/1.73 of the P-wave velocity, and velocity was assumed to be constant above the seafloor. Because the thickness of the sediment layer at the seafloor and base rock velocities beneath stations usually varies spatially, we applied an iterative station correction method several times to correct for differences in site conditions (Iwasaki et al. 1991; Sakai et al. 2005; Nakata et al. 2016). First, the correction was done by adding the time difference of S phase by sedimentary layer from the arrival-time difference between the PS and P phases (Table 1). After second time, the corrections were applied to both P and S phases. We adopted the seventh result of the iterative station correction method (see Additional file 1 for details). The standard deviations and station-correction values at this time are shown in Table 1. We adopted the 269 hypocenters within the observation network. We also tried the HypoDD method (Waldhauser and Ellsworth 2000) for comparison. Though clustered hypocenters tended to become compact, we could not get a enough number of reliable hypocenter locations for sparsely distributed ones with the HypoDD method.

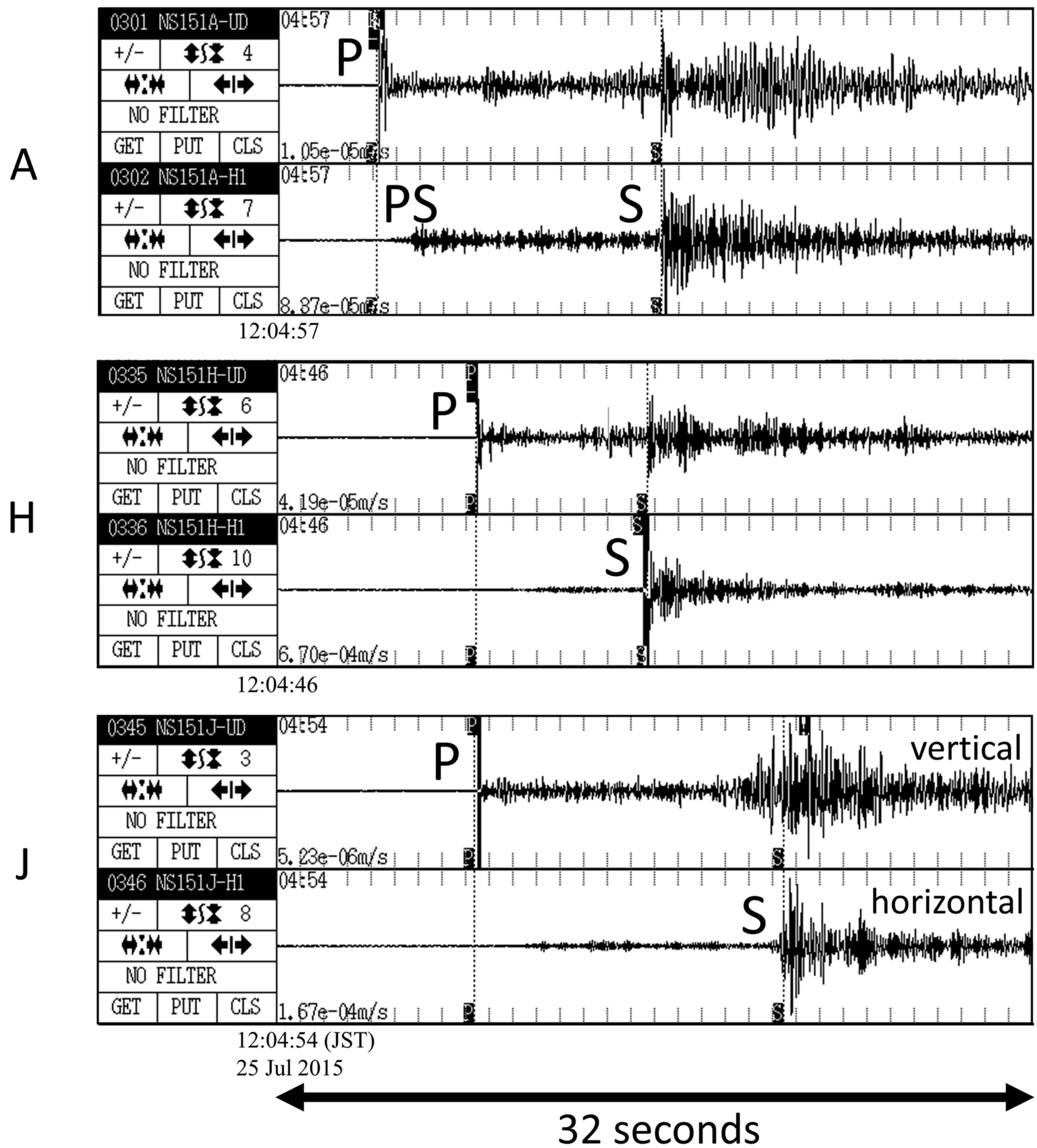

Fig. 2 Examples of seismograms observed by OBSs A, H, and J

Seismic activity in the Ogasawara region

The hypocenter distribution results obtained in this study for the Ogasawara region, including the magnitude-time diagram and the magnitude-frequency distribution (Fig. 4, Table 1), can be summarized as follows:

(1) Seismic activity was stationary during the observation period, and no swarm activity was recognized (Fig. 4b).

(2) The lower limit of detectable magnitude was about 2.0. The best-fit line for the magnitude-frequency distribution (Gutenberg and Richter 1944) had an estimated *b*-value of 0.72 (Fig. 4c). Here, the best-fit line was deduced from the maximum likelihood methods in the range of M 2.2 to 5.3.

(3) Seismicity related to the subducting PAC was recognized when the hypocenters were projected onto an east–west cross section (Fig. 4a). Double seis-

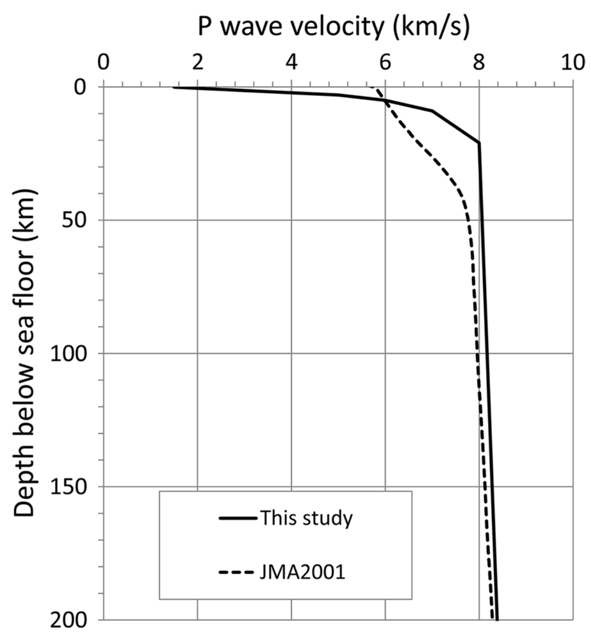

Fig. 3 One-dimensional P-wave velocity model used for hypocenter determination derived from Takahashi et al. (2009). For comparison, the velocity model used by JMA2001 (Ueno et al. 2002) is also shown

mic zone (DSZ) activity observed along the subducting slab (red circles, upper plane; blue circles, lower plane) is similar to that observed beneath the Tohoku area. The plate configuration inferred by Hayes et al. (2012) at 27.3°N, shown by a dotted line on the cross section, corresponds well to the activity observed along the upper plane.

(4) Some earthquakes were also distributed at about 20–50 km depth in the mantle wedge (green circles in Fig. 4a).

Double seismic zone (DSZ)

Seismicity was observed along two planes in the depth range from 70 to 200 km (Fig. 4a). The slab-normal distance between the two planes was 30–35 km, similar to corresponding distances observed along the Japan and Mariana trenches (Umino and Hasegawa 1975; Hosono and Yoshida 2001; Yoshida and Hosono 2002; Nakajima et al. 2009; Shiobara et al. 2010). In general, DSZs are considered to relate to pressure and thermal conditions within a subducting plate, with the upper and lower planes attributable to dehydration of the oceanic crust and of mantle serpentinite, respectively (e.g., Yamasaki and Seno 2003; Seno 2009). The relationship between the slab-normal distance obtained in this study and plate age (145.3 Ma, Syracuse et al. 2010) in the Ogasawara region is consistent with the observed global trend that slab-normal distances increase with plate age (Brudzinski et al. 2007). The DSZ is recognizable down to at least 200 km (Fig. 4a), but its extension to depths below 200 km cannot be confirmed because those depths are not covered by the observation network. Wei et al. (2017) showed that, globally, the maximum depth of DSZs is positively correlated with the thermal parameter calculated by multiplying the vertical subduction speed by plate age (Kirby et al. 1996). The relationship between the maximum depth obtained in this study and the thermal parameter in the Ogasawara region (40.8 km, Syracuse et al. 2010) is consistent with results compiled by Wei et al. (2017).

Clusters of hypocenters are recognized at 60–80 km depth in the upper plane (α and β on the map view in Fig. 4a). Kita et al. (2006) found a seismic belt at depths 70–100 km in the upper plane beneath northeast Japan, which is related to dehydration reaction in the oceanic crust. The clusters in Fig. 4 are distributed in the same depth range of the seismic belt found beneath northeast Japan. The clusters may correspond to the southward extension of the seismic belt beneath northeast Japan. The depth range of the seismic belt varies according to thermal condition (Kita et al. 2010). The relatively shallow depths of the seismic belt in the Ogasawara region may indicate the absence of such low-temperature materials seen beneath Hokkaido area.

Only 11 earthquakes were observed in the lower plane of the DSZ. Similarly, in the DSZ in the Tohoku area, less seismicity is observed in the lower plane compared with the upper plane (Hosono and Yoshida 2001). According to Umino and Hasegawa (1975), a down-dip extension-type focal mechanism is dominant in the lower plane. We tried to estimate a composite focal mechanism using data from all 11 earthquakes in the lower plane, but we obtained no clear result.

Seismicity in the mantle wedge

Some seismic activity was observed in the 20–50 km depth range inside the mantle wedge (green circles in Fig. 4a). These earthquakes, which are distributed in a wide area without forming any clusters, are located beneath the Ogasawara Trough, a forearc basin (e.g., Takahashi et al. 2009) between the current volcanic arc and the Ogasawara ridge. The seismic records of one of these earthquakes are shown in Fig. 5, and they indicate no special features such as low frequency or long duration. Active seismicity in the mantle wedge has also been observed in areas with complex plate configurations such as southern Hokkaido or the Kanto area of Japan. In the Hokkaido area, the Kuril and northeast Japan arcs are colliding (e.g., Kimura 1996), and beneath the Kanto area, the Pacific and Philippine Sea plates interact as they

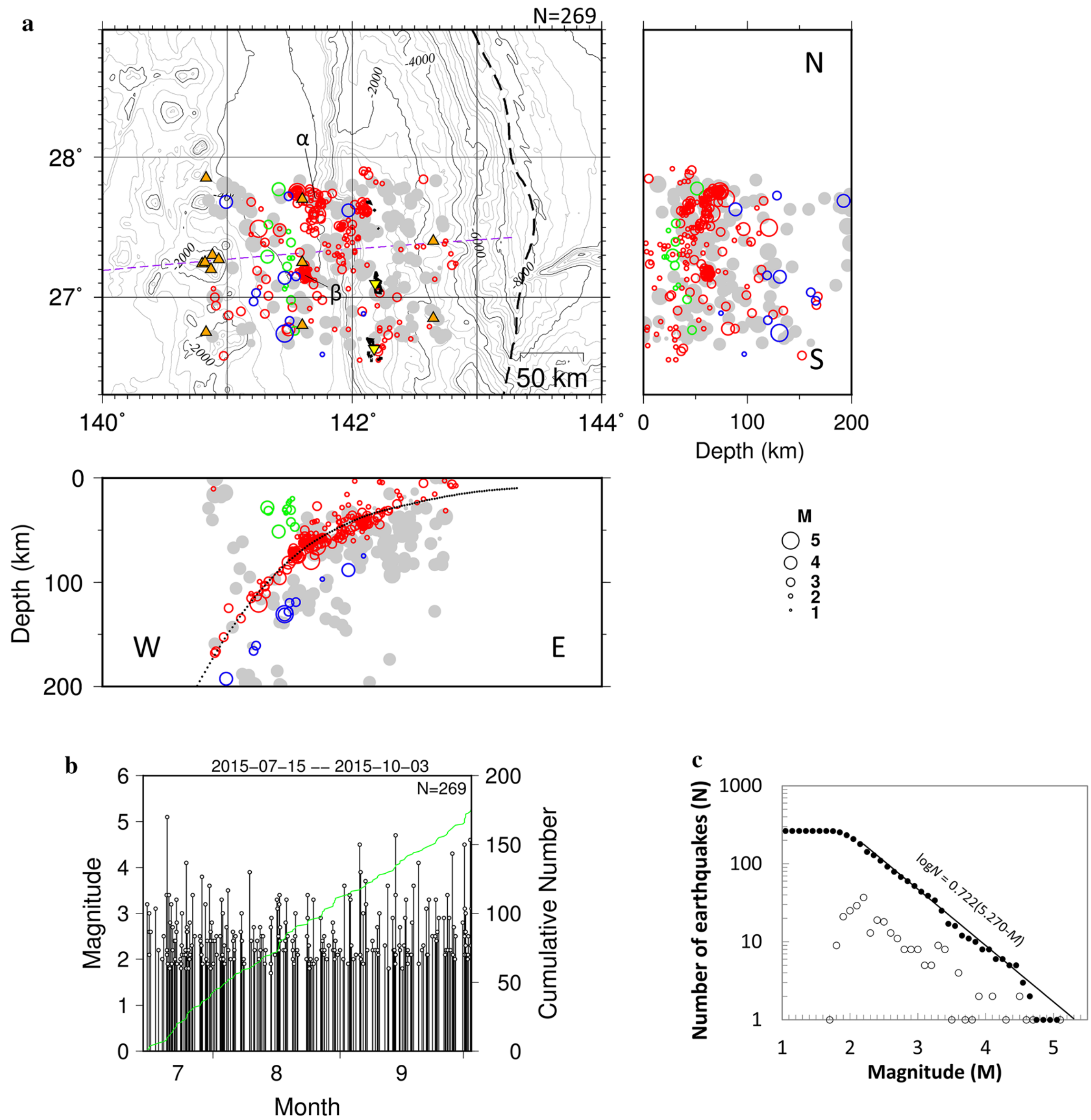

Fig. 4 Hypocenters determined in this study. **a** Map view and N–S and E–W vertical cross sections showing the hypocenter distribution (open circles) determined from the data recorded by OBSs (orange triangles) and the two island stations (inverted yellow triangles) from 15 July to 10 October 2015. The diameters of the circles indicating hypocenters vary according to the magnitude of the earthquake. Hypocenters in the upper seismic zone are shown by red circles, and those in the lower seismic zone by blue circles. Hypocenters away from the plate boundary are shown by green circles. SBJ hypocenters determined with high precision from January 2002 to December 2017 around the deployment area of the OBSs are also shown by solid gray circles. The dashed purple line in the map view shows the survey line of Takahashi et al. (2009). The dotted black line in the E–W cross section indicates the upper surface of the Pacific slab along 27.3°N, as determined by Hayes et al. (2012). α and β indicate two clusters of hypocenters at 60–80 km depth. **b** Magnitude-time diagram. The green line shows the cumulative number of earthquakes with M 2.2 or greater. **c** Magnitude–frequency distribution. Open circles denote the number of earthquakes in each magnitude bin, and solid circles show the cumulative number of earthquakes. The best-fit line according to the Gutenberg–Richter law is also shown (Gutenberg and Richter 1944)

both subduct beneath the Kanto area (e.g., Ishida 1992; Yoshida and Hosono 2002). However, seismic activity is usually low in the mantle wedge in areas without complex plate interactions, with some exceptions. For example, Uchida et al. (2010) found seismicity at depths of 25–50 km above repeating earthquakes at the plate boundary. Davey and Ristau (2011) suggested that fluid produced by dehydration of serpentine in the mantle wedge is related to the seismicity observed in the mantle wedge beneath northeast New Zealand. Laigle et al.

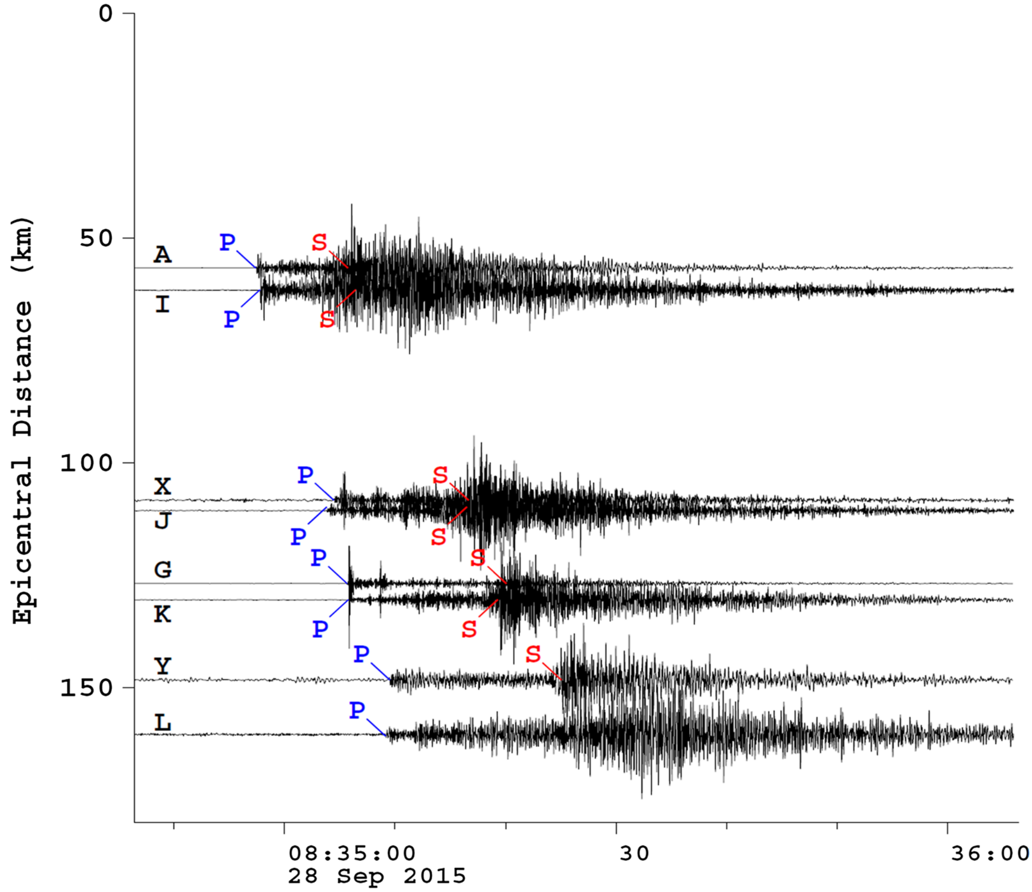

Fig. 5 Vertical seismic records of an earthquake in the mantle wedge, with the P- and S-wave arrival time picks used for hypocenter determination indicated

(2013) reported seismicity in the mantle wedge along the Lesser Antilles subduction zone. The seismicity in the mantle wedge beneath Lesser Antilles is distributed over trench-normal distance more than 50 km, which is wider than that seen in Fig. 4a. Depth ranges and sparse distribution seem similar between Ogasawara region and Lesser Antilles. Supraslab earthquakes offshore Sanriku (Uchida et al. 2010) are distributed mainly near the toe of the mantle wedge, and form clusters. Earthquakes in the mantle wedge beneath northeast New Zealand (Davey and Ristau, 2011) form clusters near the boundary of subducting slab. The seismicities offshore Sanriku and beneath northeast New Zealand look different from the seismicities around Ogasawara Islands and Lesser Antilles.

The tectonic features of the forearc basin in the Lesser Antilles and Ogasawara Island regions are similar. Thus, seismicity in the mantle wedge may be a feature of forearc basin formation, and serpentine dehydration might account for the seismic activity in the mantle wedge in the Ogasawara region. Ogasawara Islands was formed with volcanic activities in 41–48 Ma related to the beginning of the Pacific plate subduction in this area (Ishizuka et al. 2006). The backarc basin of the Lesser Antilles, Grenada basin, and the forearc basin, Tobada basin, were formed as a single structure, and the Lesser Antilles were formed by volcanic activities with dividing the single basin into the two (Aitken et al. 2011). The volcanic activity started at about 40 Ma (Briden et al. 1979) due to the rollback of the Atlantic oceanic slab subduction (Aitken et al. 2011). Both Ogasawara Trough and Tobada basin are related to the beginning of oceanic slab subduction. The seismic activity in mantle wedge may be related to dehydration of minerals which were formed at the time of subduction onset.

Comparison with SBJ and PDE locations

We compared the hypocenter locations in this study with SBJ and USGS PDE locations (Fig. 6 and Table 2). We considered earthquakes with an origin time difference less than 3.0 s to be the same earthquake. SBJ hypocenters are categorized into "high-precision hypocenters"

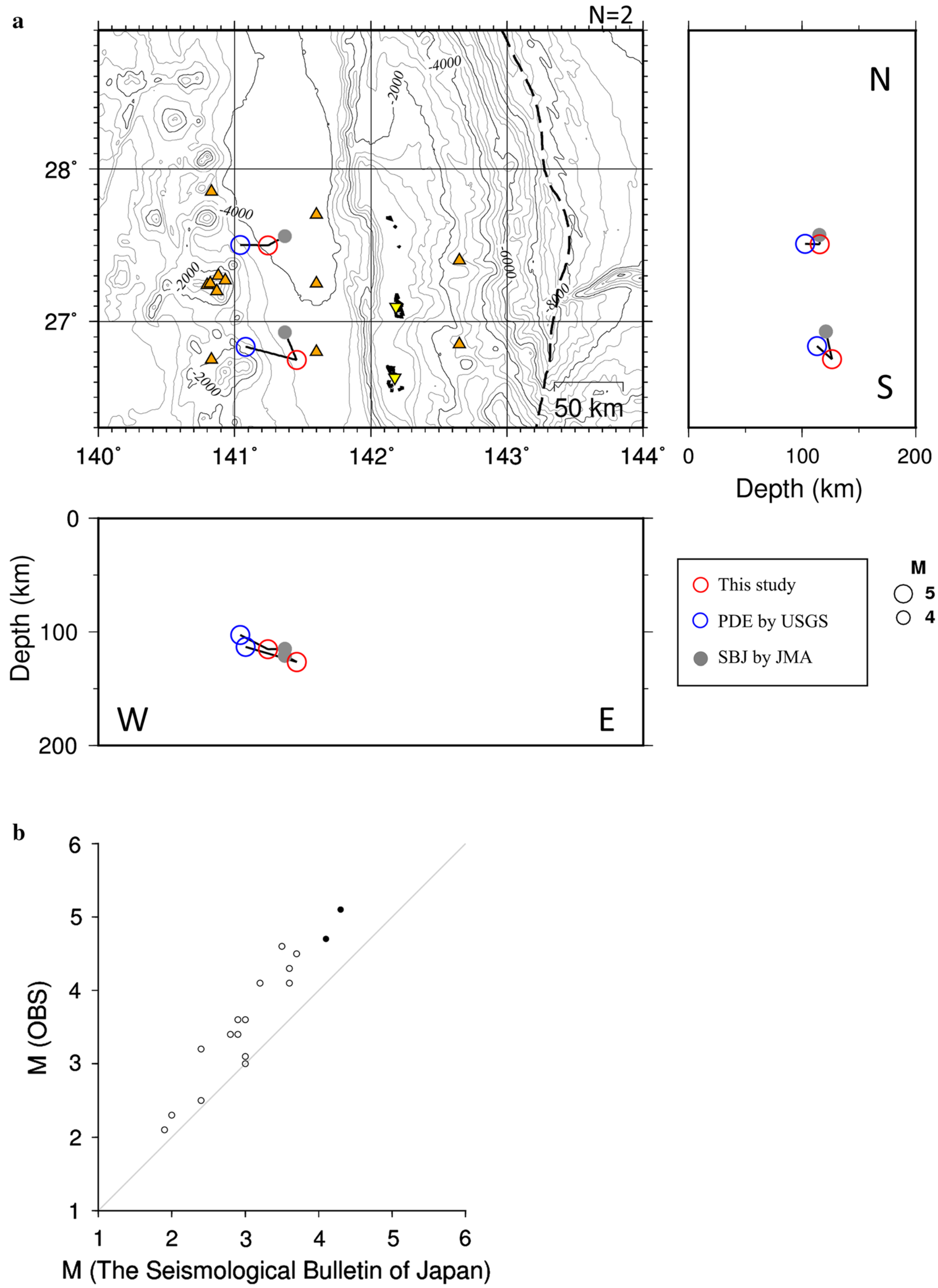

Fig. 6 Comparison of hypocenters. **a** Map view and N–S and E–W vertical cross sections comparing SBJ hypocenters (gray circles) with corresponding hypocenters determined in this study (open red circles) and PDE by the USGS (open blue circles). **b** Relationship between magnitudes determined in this study and SBJ magnitudes. Open and filled circles denote low- and high-precision SBJ hypocenters, respectively

and "low-precision hypocenters" according to hypocenter determination errors (JMA 2019). In the Ogasawara region, the locations of hypocenters in the latter category are uncertain because of the small number of used observation stations which are unevenly distributed. The magnitudes of the earthquakes with low-precision

Table 2 Comparison between SBJ hypocenters and those of this study

No.	Seismological Bulletin of Japan (1)						This study (2)					Onset time difference (1)–(2) (s)	Location difference (1)–(2) (km)	Depth difference (1)–(2) (km)
	Origin time[a] (JST)	Lat. (N) (°)	Long. (E) (°)	Depth (km)	Magnitude	Flag[b]	Origin time[a] (JST)	Lat. (N) (°)	Long. (E) (°)	Depth (km)	Magnitude			
1	2015/07/20 20:53:13.62	27.56	141.37	115	4.3		2015/07/20 20:53:12.31	27.50	141.25	115	5.1	1.31	14	0
2	2015/07/25 12:04:46.21	27.46	142.92	7	3.6	S	2015/07/25 12:04:45.66	27.71	141.78	55	4.1	0.55	129	−48
3	2015/07/27 01:30:56.34	26.93	142.33	32	2.8	S	2015/07/27 01:30:55.30	26.91	142.07	29	3.4	1.04	29	3
4	2015/07/29 04:39:02.43	26.71	142.44	28	2.0	S	2015/07/29 04:39:02.30	26.69	142.26	26	2.3	0.13	20	2
5	2015/07/31 04:37:07.26	27.29	142.20	97	3.0	S	2015/07/31 04:37:06.03	27.30	141.32	23	3.6	1.23	98	74
6	2015/08/03 10:07:07.93	27.19	140.85	26	3.0	S	2015/08/03 10:07:08.31	27.19	141.24	109	3.0	−0.38	43	−83
7	2015/08/17 03:15:10.80	27.16	142.43	76	2.4	S	2015/08/17 03:15:09.14	27.17	141.63	60	3.2	1.66	89	16
8	2015/08/17 05:56:47.02	27.02	142.31	131	2.9	S	2015/08/17 05:56:46.23	27.01	141.33	94	3.4	0.79	109	37
9	2015/09/02 01:39:14.65	27.57	141.72	106	2.9	S	2015/09/02 01:39:13.60	27.48	141.42	91	3.6	1.05	34	15
10	2015/09/05 19:06:22.19	27.70	141.78	83	3.7	S	2015/09/05 19:06:20.56	27.75	141.56	68	4.5	1.64	25	15
11	2015/09/14 12:47:45.24	26.93	141.37	121	4.1		2015/09/14 12:47:43.96	26.75	141.46	126	4.7	1.28	19	−5
12	2015/09/20 01:39:07.46	27.65	142.63	86	3.2	S	2015/09/20 01:39:05.76	27.75	141.55	68	4.1	1.70	120	18
13	2015/09/22 05:30:44.80	26.76	142.34	16	1.9	S	2015/09/22 05:30:42.90	26.73	142.36	9	2.1	1.90	3	7
14	2015/09/28 08:34:47.75	27.73	142.55	89	3.6	S	2015/09/28 08:34:46.32	27.77	141.41	46	4.3	1.43	127	43
15	2015/09/29 02:36:42.81	27.02	142.37	24	2.4	S	2015/09/29 02:36:41.52	27.01	142.36	21	2.5	1.29	1	3
16	2015/10/02 18:17:21.24	27.79	141.96	86	3.5	S	2015/10/02 18:17:20.68	27.70	141.66	74	4.6	0.56	34	12
17	2015/10/02 23:46:25.35	26.69	142.44	29	3.0	S	2015/10/02 23:46:24.61	26.62	142.20	32	3.1	0.74	27	−3

[a] Format: Year/Month/Day Hour:Minutes:Seconds

[b] Earthquakes for which the hypocenters were determined with low precision are flagged with an "S"

Table 3 Comparison between PDE hypocenters and those of this study

No.	PDE (1)					This study (2)					Onset time difference (1)–(2) (s)	Location difference (1)–(2) (km)	Depth difference (1)–(2) (km)
	Origin time[a] (JST)	Lat. (N) (°)	Long. (E) (°)	Depth (km)	Magnitude	Origin time[a] (JST)	Lat. (N) (°)	Long. (E) (°)	Depth (km)	Magnitude			
1	2015/07/20 20:53:12.88	27.50	141.04	103	4.6	2015/07/20 20:53:12.31	27.50	141.25	115	5.1	0.57	23	− 12
2	2015/09/14 12:47:43.35	26.83	141.08	113	4.5	2015/09/14 12:47:43.96	26.75	141.46	126	4.7	− 0.61	43	− 13

[a] Format: Year/Month/Day Hour:Minutes:Seconds

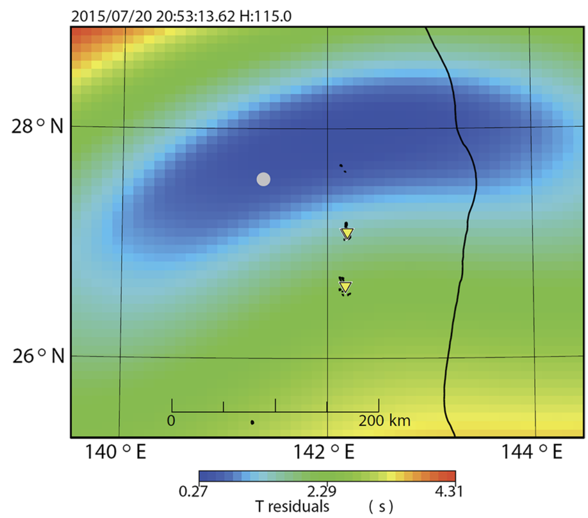

Fig. 7 An example of the travel-time residual distribution of an earthquake in SBJ. The gray circle indicates the hypocenter location, and the inverted yellow triangles show the locations of three stations situated on islands

hypocenters are generally smaller than the others. Only two high-precision SBJ hypocenters matched with our OBS hypocenters (connected by lines in Fig. 6a), and the SBJ and OBS hypocenter locations were a few tens of km apart. Fifteen low-precision hypocenters (flagged with "S" in Table 2) also matched with OBS hypocenters. When all 17 earthquakes are considered, the distances between SBJ and OBS hypocenter locations are distributed from a few km to over 100 km.

We also compared the locations of two OBS hypocenters with the PDE locations estimated for the same earthquakes (Table 3) and found that the PDE hypocenters were about 30 km west of the OBS hypocenters. These two earthquakes were same as those matched with SBJ. The high-precision SBJ hypocenter locations were closer to the OBS than the PDE, although there were only two data. When we compared the hypocenter locations of the SBJ and the PDE occurring over a 1-year period (Fig. 1), we found that the difference between them is remarkable in the east–west direction. The SBJ earthquake locations were estimated by using onset times obtained at Chichijima, Hahajima, Iwoto, and stations on distant main islands of Japan. The PDE earthquake locations were estimated by them at Chichijima, some stations on main islands of Japan, and distant stations around the world. The distribution of travel-time residuals for an earthquake occurring at 20:53:13 20 July 2015 in the SBJ data (Fig. 7) shows an area with small residuals with an east–west orientation, and the resolution of hypocenters is considered to be poor in the east–west direction. This is considered to be a cause of the hypocenter difference in the east–west direction.

We also examined the relationship between OBS magnitudes and SBJ magnitudes (Fig. 6b), including those of the low-precision SBJ hypocenters. We consider the precision of the hypocentral distances used in magnitude determination to be reliable because the hypocentral distance is constrained by the observed P–S time difference even if data are available from only a few stations. The greater magnitudes of this study, which are higher by 0.5 relative to the SBJ magnitudes (Fig. 6b), can be attributed to amplification by the soft sediment layers beneath the OBS stations (Aoki and Yoshida 2005).

Conclusions

A seismic observation by ocean bottom seismometers in 2015 revealed some notable features of seismicity in the Ogasawara region.

(1) Seismicity relating to the subduction of the Pacific plate (PAC) was observed, and a double seismic zone (DSZ) was observed in the 70–200 km depth range. The distribution of seismicity is mostly consistent with the plate model proposed by Hayes et al. (2012).
(2) Seismic activity observed within the mantle wedge, above the seismicity of the PAC, may be related to onset of the oceanic slab subduction.
(3) *Seismological Bulletin of Japan* locations seem to be a few tens of kilometers apart from the locations determined in this study. USGS locations (Preliminary Determination of Epicenters) seem to be offset westward about 30 km compared with the locations determined in this study.

Additional file

Additional file 1. Additional figures showing the process of hypocenter determination by iterative station corrections.

Abbreviations
DSZ: double seismic zone; JMA: Japan Meteorological Agency; OBS: ocean bottom seismometer; PAC: Pacific plate; PDE: Preliminary Determination of Epicenters; PHS: Philippine Sea plate; SBJ: Seismological Bulletin of Japan; STA: short-term-average; LTA: long-term-average; USGS: United States Geological Survey.

Authors' contributions
KN conducted the observation, analyzed the OBS seismic records, and wrote most of the manuscript. AKo suggested improvements to the observation plan, picked the seismic records, and helped with the preparation of the manuscript. AKa contributed to the observation plan and data analysis and wrote the section on "Seismicity in the mantle wedge". FH contributed to the

"Double Seismic Zone" section and offered suggestions about the organization of the manuscript. KK conducted onboard operations. TN contributed to the "Comparison with the Location of SBJ" section and the data analysis. HT contributed to the observation and data analysis. KM contributed to the observation plan. HB, NH, CY, and MK helped conduct onboard OBS operations and analyzed some seismic records. All authors read and approved the final manuscript.

Author details
[1] Meteorological Research Institute, Japan Meteorological Agency, 1-1 Nagamine, Tsukuba, Ibaraki 305-0052, Japan. [2] Seismology and Volcanology Department, Japan Meteorological Agency, 1-3-4 Otemachi, Chiyoda-ku, Tokyo 100-8122, Japan. [3] School of Marine Science and Technology, Tokai University, 3-20-1 Orido, Shimizu-ku, Shizuoka 424-8610, Japan. [4] NC Geophysical Survey Co., LTD., 658-2 Hongo-cho, Funabashi, Chiba 273-0033, Japan. [5] Fukken Co., LTD., 2-10-11 Hikari-cho, Higashi-ku, Hiroshima 732-0052, Japan. [6] Japan Drilling Co., LTD., 2-4-3 Nihonbashi Horidome-cho, Chuo-ku, Tokyo 103-0012, Japan.

Acknowledgements
The observation was conducted with the cooperation of the Japan Meteorological Agency (JMA) research vessel *Keifu-Maru* and the Global Environment and Marine and the Seismology and Volcanology departments of JMA. We used the WIN system by Urabe and Tsukada (1992) for analysis of the seismic records and HYPOMH software (Hirata and Matsu'ura 1987) for hypocenter determination. HypoDD code (https://www.ldeo.columbia.edu/~felixw/hypoDD.html) was used for hypocenter determination. We used hypocenters of earthquakes from January 2002 to December 2017 in the *Seismological Bulletin of Japan*. SBJ is published by Japan Meteorological Agency with the cooperation of the Ministry of Education, Culture, Sports, Science and Technology of Japan and uses data from the National Research Institute for Earth Science and Disaster Prevention, Hokkaido University, Hirosaki University, Tohoku University, The University of Tokyo, Nagoya University, Kyoto University, Kochi University, Kyushu University, Kagoshima University, the National Institute of Advanced Industrial Science and Technology, the Geospatial Information Authority of Japan, the Japan Agency for Marine-Earth Science and Technology, the Association for the Development of Earthquake Prediction, the governments of Aomori Prefecture, the Tokyo Metropolitan Area, Shizuoka Prefecture, and Kanagawa Prefecture, the Incorporated Research Institutes for Seismology, and the Japan Meteorological Agency. Some figures were drawn with Generic Mapping Tools (Wessel and Smith 1998). We thank Editor Kyoko Okino and two anonymous reviewers for their thorough reviews and valuable suggestions on improving the quality of this article.

Competing interests
The authors declare that they have no competing interests.

Availability of data and materials
SBJ by JMA is available at http://www.data.jma.go.jp/svd/eqev/data/bulletin/. PDE by USGS is available at https://earthquake.usgs.gov/data/pde.php. The data used in this study are available from the corresponding author on request.

Funding
This research was conducted with support from the Japan Meteorological Agency and the research fund of Tokai University.

Publisher's Note

Springer Nature remains neutral with regard to jurisdictional claims in published maps and institutional affiliations.

Received: 6 November 2018 Accepted: 6 March 2019
Published online: 11 March 2019

References
Aitken T, Mann P, Escalona A, Christeson GL (2011) Evolution of the Grenada and Tobago basins and implications for arc migration. Mar Pet Geol 28:235–258. https://doi.org/10.1016/j.marpetgeo.2009.10.003
Aoki G, Yoshida Y (2005) Seismicity observed by pop-up OBSs off Tokai region. Tech Rep Meteorol Res Inst 46:1–31 **(in Japanese)**
Briden JC, Rex DC, Faller AM, Tomblin JF (1979) K-Ar geochronology and paleomagnetism of volcanic rocks in the Lesser Antilles island arc. Philos Trans R Soc Lond Ser A 291:485–528. https://doi.org/10.1098/rsta.1979.0040
Brudzinski MR, Thurber CH, Hacker BR, Engdahl ER (2007) Global prevalence of double Benioff zones. Science 316:1472–1474. https://doi.org/10.1126/science.1139204
Davey FJ, Ristau J (2011) Fore-arc mantle wedge seismicity under northeast New Zealand. Tectonophysics 509:272–279. https://doi.org/10.1016/j.tecto.2011.06.017
Gutenberg B, Richter CF (1944) Frequency of earthquakes in California. Bull Seismol Soc Am 34:185–188
Hayes GP, Wald DJ, Johnson RL (2012) Slab1.0: a three-dimensional model of global subduction zone geometries. J Geophys Res 117:B01302. https://doi.org/10.1029/2011jb008524
Hirata N, Matsu'ura M (1987) Maximum-likelihood estimation of hypocenter with origin time eliminated using nonlinear inversion technique. Phys Earth Planet Inter 47:50–61. https://doi.org/10.1016/0031-9201(87)90066-5
Hosono K, Yoshida A (2001) Volcanic front and intermediate-depth seismicity in northeastern Japan. Bull Volcanol Soc Jpn 46:305–316. https://doi.org/10.18940/kazan.46.6_305 **(in Japanese with English abstract)**
Ishibashi K, Harada T (2013) Working hypothesis of the 1605 Great Izu–Bonin Trench Earthquake and the 1614 Nankai Trough earthquake. In: Programme and Abstracts, The Seismological Society of Japan 2013 Fall Meeting, D21-03 **(in Japanese)**
Ishida M (1992) Geometry and relative motion of the Philippine Sea plate and Pacific plate beneath the Kanto-Tokai district, Japan. J Geophys Res 97:489–513. https://doi.org/10.1029/91JB02567
Ishizuka O, Kimura J, Li YB, Stern RJ, Reagan MK, Taylor RN, Ohara Y, Bloomer SH, Ishii T, Hargrove US III, Haraguchi S (2006) Early stages in the evolution of Izu–Bonin arc volcanism: new age, chemical and isotopic constrains. Earth Planet Sci Lett 250:385–401. https://doi.org/10.1016/j.epsl.2006.08.007
Iwasaki T, Hirata N, Kanazawa T, Urabe T, Motoya Y, Shimamura H (1991) Earthquake distribution in the subduction zone off eastern Hokkaido, Japan, deduced from ocean-bottom seismographic and land observations. Geophys J Int 105:693–711. https://doi.org/10.1111/j.1365-246X.1991.tb00806.x
Japan Meteorological Agency (2010) Monthly report on earthquakes and volcanoes in Japan. http://www.data.jma.go.jp/svd/eqev/data/gaikyo/monthly/201012/monthly201012.pdf. Accessed 20 Nov 2017
Japan Meteorological Agency (2015) Monthly report on earthquakes and volcanoes in Japan. http://www.data.jma.go.jp/svd/eqev/data/gaikyo/monthly/201505/201505monthly.pdf. Accessed 20 Nov 2017
Japan Meteorological Agency (2019) The seismological bulletin of Japan user's guide. https://www.data.jma.go.jp/svd/eqev/data/bulletin/catalog/notes_e.html. Accessed 18 Feb 2019
Kimura G (1996) Collision orogeny at arc-arc junctions in the Japanese Islands. Isl Arc 5:262–275. https://doi.org/10.1111/j.1440-1738.1996.tb00031.x
Kirby S, Engdahl RE, Denlinger R (1996) Intermediate-depth intraslab earthquakes and arc volcanism as physical expressions of crustal and uppermost mantle metamorphism in subducting slabs. In: Bebout GE, Scholl DW, Kirby SH, Platt JP (eds) Subduction top to bottom. Geophysical monograph, vol 96. AGU, Washington, pp 195–214. https://doi.org/10.1029/gm096p0195
Kita S, Okada T, Nakajima J, Matsuzawa T, Hasegawa A (2006) Existence of a seismic belt in the upper plane of the double seismic zone extending in the along-arc direction at depths of 70–100 km beneath NE Japan. Geophys Res Lett 33:L24310. https://doi.org/10.1029/2006GL028239
Kita S, Okada T, Hasegawa A, Nakajima J, Matsuzawa T (2010) Anomalous deepening of a seismic belt in the upper-plane of the double seismic zone in the Pacific slab beneath the Hokkaido corner: possible evidence for thermal shielding caused by subducted forearc crust materials. Earth Planet Sci Lett 290:415–426. https://doi.org/10.1016/j.epsl.2009.12.038
Kodaira S, Noguchi N, Takahashi N, Ishizuka O, Kaneda Y (2010) Evolution from fore-arc oceanic crust to island arc crust: a seismic study along the Izu–Bonin fore arc. J Geophys Res 115:B09102. https://doi.org/10.1029/2009JB006968

Laigle M, Hirn A, Sapin M, Bécel A, Charvis P, Flueh E, Diaz J, Lebrun JF, Gesret A, Raffaele R, Galvé A, Evain M, Ruiz M, Kopp H, Bayrakci G, Weinzierl W, Hello Y, Lépine JC, Viodé JP, Sachpazi M, Gallart J, Kissling E, Nicolich R (2013) Seismic structure and activity of the north-central Lesser Antilles subduction zone from an integrated approach: similarities with the Tohoku forearc. Tectonophysics 603:1–20. https://doi.org/10.1016/j.tecto.2013.05.043

Nakajima J, Hirose F, Hasegawa A (2009) Seismotectonics beneath the Tokyo metropolitan area, Japan: effect of slab-slab contact and overlap on seismicity. J Geophys Res 114:B08309. https://doi.org/10.1029/2008JB006101

Nakata K, Kobayashi A, Hirata K, Tsushima H, Yamazaki A, Katsumata A, Maeda K, Baba H, Ichinose S, Ushida T, Ishihara T, Inamura K, Hasuzawa T (2016) Seismicity within the Philippine Sea plate south of the Nankai trough axis off the Kii Peninsula: estimates from ocean bottom seismographic data in 2013 and 2014. Zisin2 69:59–68. https://doi.org/10.4294/zisin.69.59 **(in Japanese with English abstract)**

Sakai S, Yamada T, Shinohara M, Hagiwara H, Kanazawa T, Obana K, Kodaira S, Kaneda Y (2005) Urgent aftershock observation of the 2004 off the Kii Peninsula earthquake using ocean bottom seismometers. Earth Planets Space 57:363–368. https://doi.org/10.1186/BF03352577

Scholz CH, Small C (1997) The effect of seamount subduction on seismic coupling. Geology 25:487–490. https://doi.org/10.1130/0091-7613(1997)025%3c0487:TEOSSO%3e2.3.CO;2

Seno T (2009) Intraslab seismicity and its generation mechanisms. Zisin2 61:S357–S364. https://doi.org/10.4294/zisin.61.357 **(in Japanese with English abstract)**

Shiobara H, Sugioka H, Mochizuki K, Oki S, Kanazawa T, Fukao Y, Suyehiro K (2010) Double seismic zone in the North Mariana region revealed by long-term ocean bottom array observation. Geophys J Int 183:1455–1469. https://doi.org/10.1111/j.1365-246X.2010.04799.x

Syracuse EM, van Keken PE, Abers GA (2010) The global range of subduction zone thermal models. Phys Earth Planet Inter 183:73–90. https://doi.org/10.1016/j.pepi.2010.02.004

Takahashi N, Kodaira S, Tatsumi Y, Yamashita M, Sato T, Kaiho Y, Miura S, No T, Takizawa K, Kaneda Y (2009) Structural variations of arc crusts and rifted margins in the southern Izu-Ogasawara arc–back arc system. Geochem Geophys Geosyst 10:Q09X08. https://doi.org/10.1029/2008gc002146

Uchida N, Kirby SH, Okada T, Hino R, Hasegawa A (2010) Supraslab earthquake clusters above the subduction plate boundary offshore Sanriku, northeastern Japan: seismogenesis in a graveyard of detached seamounts? J Geophys Res 115:B09308. https://doi.org/10.1029/2009JB006797

Ueno H, Hatakeyama S, Aketagawa A, Funasaki J, Hamada N (2002) Improvement of hypocenter determination procedures in the Japan Meteorological Agency. Q J Seismol 65:123–134 **(in Japanese with English abstract)**

Umino N, Hasegawa A (1975) On the two-layered structure of deep seismic plane in northeaster Japan arc. Zisin2 28:125–139. https://doi.org/10.4294/zisin1948.28.2_125 **(in Japanese with English abstract)**

Urabe T, Hirata N (1984) A playback system for long-term analog tape recordings of ocean bottom seismographs. Zisin 37:633–645. https://doi.org/10.4294/zisin1948.37.4_633 **(in Japanese and English abstract)**

Urabe T, Tsukada S (1992) Win—a workstation program for processing waveform data from microearthquake networks. Programme Abstr Seismol Soc Jpn 1992(2):331 **(in Japanese)**

Waldhauser F, Ellsworth WL (2000) A double-difference earthquake location algorithm: method and application to the Northern Hayward fault, California. Bull Seismol Soc Am 90:1352–1368. https://doi.org/10.1785/0120000006

Wei SS, Wiens DA, van Keken PE, Cai C (2017) Slab temperature controls on the Tonga double seismic zone and slab mantle dehydration. Sci Adv 3:e1601755. https://doi.org/10.1126/sciadv.1601755

Wessel P, Smith WHF (1998) New, improved version of generic mapping tools released. EOS Trans Am Geophys Union 79:579. https://doi.org/10.1029/98EO00426

Yamasaki T, Seno T (2003) Double seismic zone and dehydration embrittlement of the subducting slab. J Geophys Res 108(B4):2212. https://doi.org/10.1029/2002JB001918

Yamazaki A (2011) Pop-up ocean bottom seismometer observations in the regions along Nankai trough. Tech Rep Meteorol Res Inst 63:1–35 **(in Japanese)**

Yoshida A, Hosono K (2002) Volcanic front and intermediate-depth seismicity (the second report)—Kanto and Hokkaido regions. Bull Volcanol Soc Jpn 47:727–738. https://doi.org/10.18940/kazan.47.6_727 **(in Japanese with English abstract)**